THE LCF BEHAVIOR OF THE NI-BASE SUPERALLOY PWA 1489

IN HYDROGEN

P.S. Chen, E.J. Vesely, Jr., and B. Panda

IIT Research Institute
Metallurgy Research Facility
Marshall Space Flight Center, AL 35812

W.D. Hamilton and R.A. Parr

National Aeronautics and Space Administration
Materials and Processes Laboratory
Marshall Space Flight Center, AL 35812

Abstract

This paper summarizes the study of the effects of hydrogen on the low-cycle (LCF) and double-notch low cycle fatigue (DN-LCF) fracture characteristics of a microcast Ni-base superalloy PWA 1489. The LCF tests were conducted in fully reversed strain control mode, while DN-LCF tests were run using a stress controlled tension-tension cycle with R= 0.05. Hydrogen was found to significantly reduce the number of cycles to failure. Extensive fractography revealed that hydrogen enhanced cleavage on {100} planes during the early stage of crack propagation for both LCF and DN-LCF tests. Possible mechanisms regarding hydrogen-induced degradation of LCF life are proposed on the basis of the present findings and the known hydrogen embrittlement mechanisms for Ni-base superalloys.

Superalloys 1992
Edited by S.D. Antolovich, R.W. Stusrud, R.A. MacKay,
D.L. Anton, T. Khan, R.D. Kissinger, D.L. Klarstrom
The Minerals, Metals & Materials Society, 1992

Introduction

Ni-base superalloys are being considered for turbopump turbine blade materials in the Space Shuttle Main Engine (SSME). Many components in the turbopumps are exposed to high pressure gaseous hydrogen environment during service, therefore one of the most serious concerns is hydrogen-affected fatigue failure because the materials are subjected to cyclic loadings.

PWA 1489, a microcast MAR-M-247 Ni-base superalloy, is a candidate material for turbine blades in the high pressure alternate turbopump (ATD) for the SSME. Recently, the effects of high pressure hydrogen on the tensile properties of Ni-base superalloys have been the subject for many studies [1-8]. However, there have been very few studies on the hydrogen-affected cyclic loading of superalloys; therefore this study was undertaken to better understand the role of hydrogen on the LCF properties of PWA 1489. Fatigue fracture characteristics were studied in relation to the reduction of LCF life caused by gaseous hydrogen. The LCF properties of PWA 1489 in hydrogen are discussed in terms of total strain, maximum resultant stress and maximum stress. Possible mechanisms pertaining to the hydrogen induced fatigue life degradation are suggested based on the present findings and the existing mechanisms of hydrogen embrittlement.

Experimental Procedures

PWA 1489 specimens were furnished by Pratt & Whitney. The nominal composition of the PWA 1489 is shown in Table I.

TABLE I - Nominal Composition of PWA 1489

PWA 1489	Ni	Cr	Co	Ta	W	Ti	Al	Hf
	Bal	8.5	10	3	10	1.5	5.5	1.5

The LCF tests were conducted in fully reversed, strain control mode in 5 ksi hydrogen at ambient temperature. The specimen used for the LCF tests is shown in Figure 1. DN-LCF tests were run at room temperature using a stress controlled tension-tension cycle with R= 0.05 in both air and hydrogen. The specimen used for the DN-LCF test is shown in Figure 2. A Cambridge SEM operating at 20 kV was used to study the microstructure and fractography. The orientation of the cleavage planes was determined by trace analysis, taking into account γ' morphology and intersecting angle of slip trace [2,3].

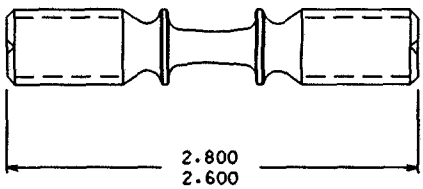

Figure 1 - Specimen design used for smooth LCF testing.

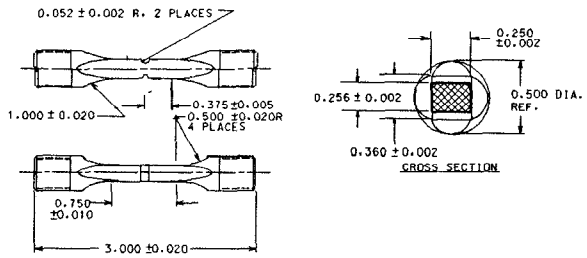

Figure 2 - Specimen design used for DN-LCF testing [9].

Results

Microstructure

PWA 1489 is a γ'-strengthened microcast Ni-base superalloy with the γ' size ranging from 0.5 to 0.8 microns. The edges of the γ' cubes were confirmed to be parallel to the $<100>$ directions of the γ matrix. The typical microstructure showing grain structure and cuboidal γ' precipitate is shown in Figure 3.

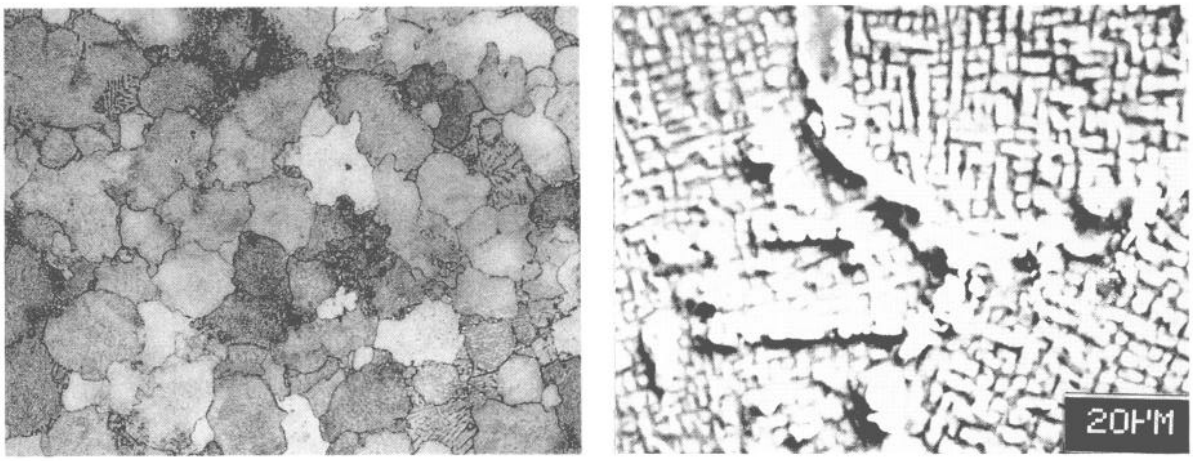

(a) (b)

Figure 3 - Microstructure of PWA 1489 showing (a) grain structure (100x) and (b) cuboidal γ' precipitate.

Fatigue Tests

A summary of LCF test results is plotted in Figure 4. The LCF tests conducted elsewhere in air are also included in Figure 4 for comparison [9]. A comparison of hysteresis loops for LCF specimens tested at three different total strains is given in Figure 5. As can be seen, a substantial amount of plastic strain was introduced in the initial cycles at 1.0% total strain. The extent of plastic strain decreased as the total strain is reduced. The cyclic-hardening response versus fatigue cycles is given in Figure 6. For the specimens tested at 1.0% and 0.8% total strain, significant cyclic-hardening was observed after early cycles and continued until final rupture. However, approximately no change in the resultant stress was observed for the specimen tested at 0.6% total strain.

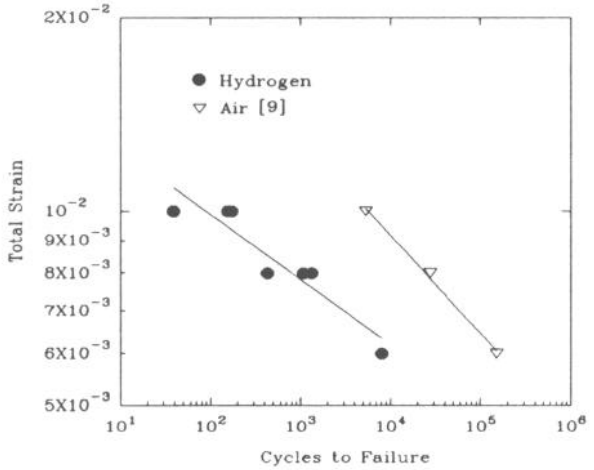

Figure 4 - Plot of LCF data for PWA 1489.

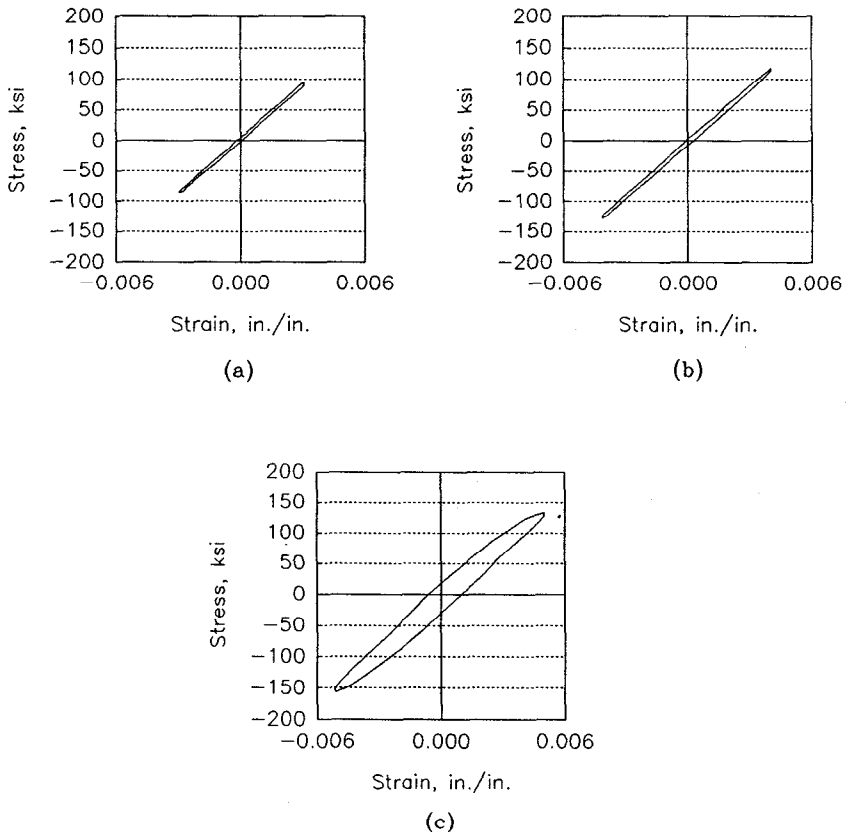

Figure 5 - Typical hysteresis loops for PWA 1489 tested in hydrogen at $\Delta\varepsilon_t$'s of (a) 0.6, (b) 0.8, and (c) 1.0%.

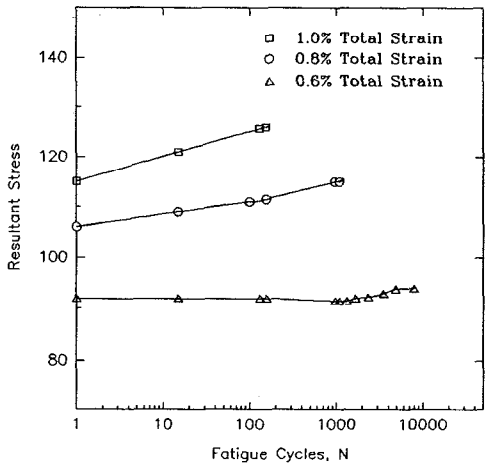

Figure 6 - LCF cyclic hardening response of PWA 1489.

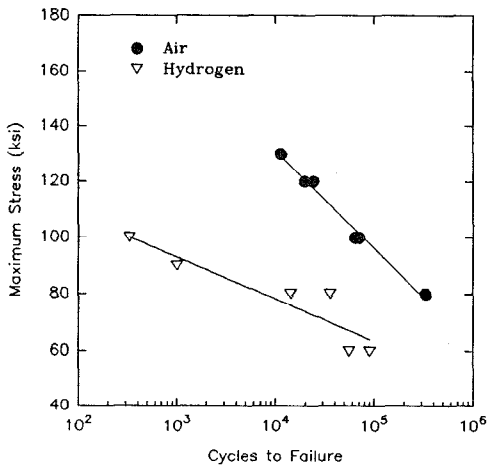

Figure 7 - Plot of LCF double-notch results for PWA 1489.

Figure 7 illustrates the results of DN-LCF tests. As shown, hydrogen has significantly reduced the DN-LCF life of PWA 1489 regardless of the stress ranges. Also the effects of hydrogen appeared to be greater at higher stress ranges.

LCF Fractography

Cleavage plane orientations near and outside the fatigue origin for all the specimens are given in Table II. As the table indicates, the fatigue crack initiated on {111} planes near the edge of the fracture surface for all the specimens. The specimen tested at 1.0% controlled strain displayed pulled-out γ' and {100} cleavage near the LCF origin (Figure 8a). At 0.8 % controlled strain, crack initiated from the {111} cleavage near the origin propagation by a combination {100} and {111} type cleavage until final rupture (Figure 8b). A substantial difference in fracture mode was observed at 0.6% controlled strain as compared to 1.0% and 0.8% controlled strain. Fatigue crack initiated at {111} plane and propagated predominately along {111} type microcleavage planes until final rupture (Figure 9). In summary, the specimens failed transgranularly on {100} cleavage; intergranular fracture was not observed.

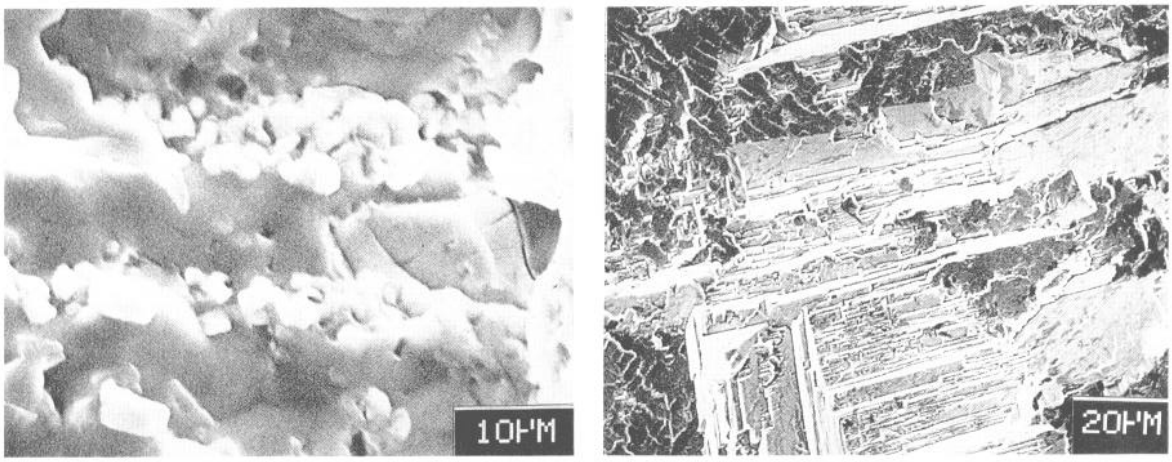

(a) (b)

Figure 8 - The fracture surface displayed (a) pulled-out γ' particles (1.0 total strain) and (b) {100} cleavage near the fatigue origin (0.8% total strain).

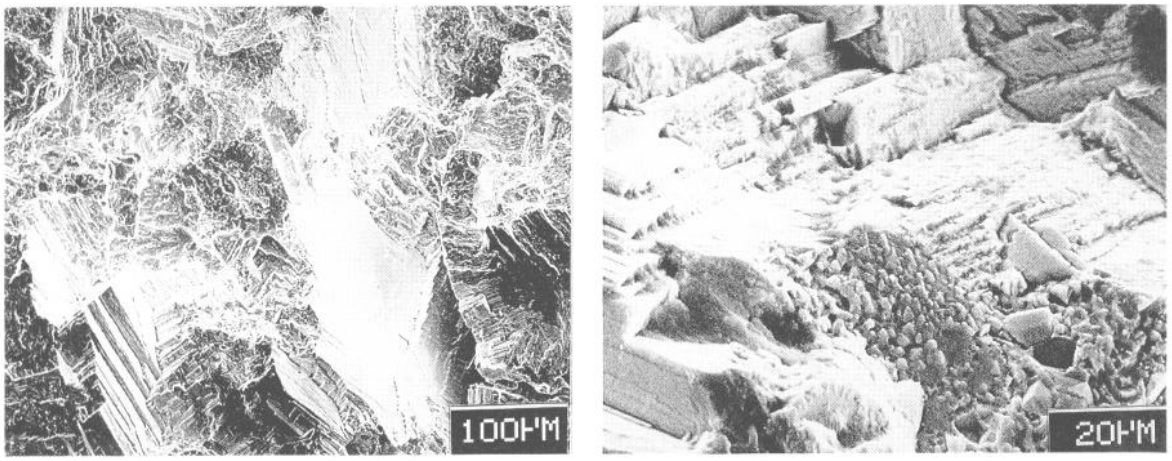

(a) (b)

Figure 9 - (a) The fatigue initiation from {111} planes near the edge of the fracture surface (b) an enlarged photograph showing details of fatigue propagation along various {111} planes (0.6% total strain).

TABLE II - LCF Fractographic Observation for PWA 1489

Testing Conditions	Control Strain	Fatigue Initiation	Near Origin	Fatigue Propagation	Final Rupture
Air; room temperature	±0.5% ±0.4% ±0.3%	{111} cleavage	{111} cleavage	{111} cleavage	{111} cleavage
5000 psi H_2 at room temperature	±0.5%	{111} cleavage	γ' pull-out & {100} cleavage	{100} cleavage	{111} cleavage
5000 psi H_2 at room temperature	±0.4%	{111} cleavage	Mainly {100} cleavage	{100} & {111} cleavage	{111} cleavage
5000 psi H^2 at room temperature	±0.3%	{111} cleavage	Mainly {100} cleavage	{100} & {111} cleavage	{111} cleavage

TABLE III - Double-Notch LCF Fractographic Observation for PWA 1489

Testing Conditions	Test Level	Fatigue Initiation	Near Origin	Fatigue Propagation	Final Rupture
5000 psi H_2 at room temperature	100 ksi R=0.05	{111} cleavage	{100} & {111} cleavage	{100} & {111} cleavage	{111} cleavage
5000 psi H_2 at room temperature	80 ksi R=0.05	{111} cleavage	{100} & {111} cleavage	{100} & {111} cleavage	{111} cleavage
5000 psi H_2 at room temperature	60 ksi R=0.05	{111} cleavage	{111} cleavage	{111} & {100} cleavage	{111} cleavage

LCF Double-Notch Testing

The cleavage plane orientations near and outside the fatigue origins are given in Table III. In air, fatigue cracks originated from {111} cleavage near the specimen surface and propagated through {111} planes regardless of the total stress range (Figure 10). There is no evidence of {100} cleavage in the specimens tested in air. In hydrogen, the fatigue crack also initiated from {111} planes near the fracture surface; however, this soon changed to a mixed mode cleavage containing {111} and {100} planes when the maximum stress is greater than 80 ksi (Figure 11). For the specimens tested at 60 ksi, {100} cleavage was not observed in the early propagation region. The DN-LCF induced fracture behavior in hydrogen can be summarized as fracture initiated from {111} and propagated along {100} and {111} cleavage planes until final rupture. The DN-LCF and smooth LCF differed in that γ' pull-out was not observed in all the DN-LCF fracture surfaces.

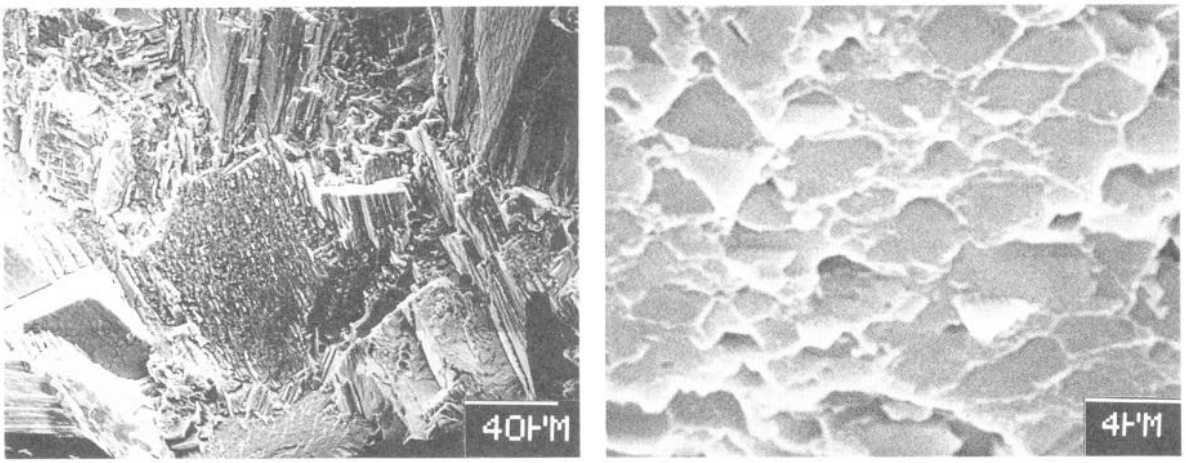

(a) (b)

Figure 10 - SEM photographs showing (a) a crack initiated from {111} planes and (b) the detailed morphology of γ' in a {111} cleavage plane near the origin.

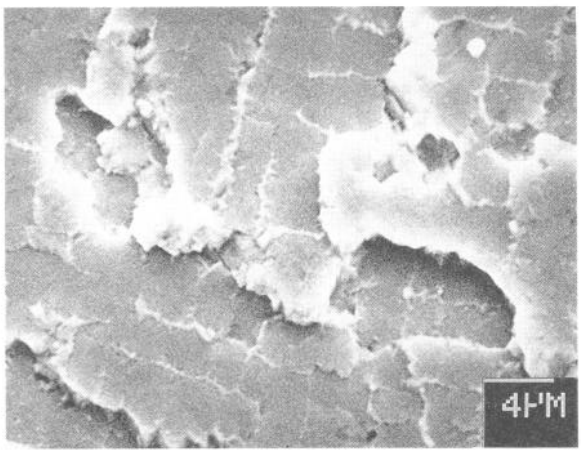

Figure 11 - SEM photographs showing the morphology of {100} cleavage plane in the specimen tested at 100 ksi in hydrogen.

Discussion

The PWA 1489 revealed a marked decrease in LCF life in hydrogen; and the influence of hydrogen on LCF appeared to correspond to a change in crack initiation and propagation. It is known that fatigue tends to generate {111} cleavage in nickel-based superalloys [10-13] in air at ambient temperature. The crack propagation along {111} slip plane is to relax the shear stress components near the crack-tip field [10,11]. This is consistent with the present DN-LCF test results in air.

However, Ni-base superalloys behave differently in hydrogen [1-8]. The studies on PWA 1480E [2,3] observed that hydrogen induced {100} cleavage regardless of the single crystal orientations. A more recent study on the LCF properties of PWA 1480 found that hydrogen promoted {100} cleavage and led to significant LCF life reduction [14]. Because of the similarity in γ' microstructure between PWA 1489 and PWA 1480, {100} cleavage found in PWA 1489 indicated hydrogen embrittlement and the mechanism proposed for LCF PWA 1480 [14] in hydrogen should be applicable to PWA 1489 with a slight modification.

The effects of hydrogen on the properties of LCF and DN-LCF are discussed and compared below.

Smooth LCF Testing

Although {100} cleavage planes were found in all the LCF specimens, there are some variations in fracture characteristics as a function of total strain range. Significant γ' pull-out was observed in the specimens tested at 1.0% total strain. When the total strain changed to 0.8% and 0.6%, γ' pull-out was not detected. Therefore, the change in the occurrence of γ' pull-out appeared to be pertinent to the maximum resultant stress, plastic deformation and cyclic- hardening. As can be seen in Figure 6, 1.0% total strain led to a resultant stress of approximately 126 ksi that is approximately 10 ksi higher than the yield strength. In addition, considerable plastic deformation and cyclic-hardening was observed for the specimens tested at 1.0% total strain (Figures 5,6). The early-stage yielding and the subsequent cyclic-hardening effects should be accountable for the hydrogen-induced γ' pull-out. Therefore, the γ' pull-out is possibly a result of very severe hydrogen embrittlement.

A possible LCF-induced fracture mechanism could be modelled in accordance with the fracture characteristics and the known HEE mechanisms. During the early stage of LCF testing, a localized stress facilitated crack initiation. A crack was initiated at a micropore or {111} cleavage plane due to stress concentration. During the early stages of crack propagation, larger stress was required to advance the crack because of smaller crack size. Therefore, the area around the fatigue crack origin must have high dislocation density within the narrow γ matrix. The slower advancing rate in the early stage of propagation led to more extensive dislocation entanglement in the narrow γ region which, in turn, favored a crack propagation along {100} γ/γ' interfacial region. Higher strain amplitudes tended to enhance more dislocation entanglement near the γ/γ' interface because of the higher resultant stresses. When dislocation became too tangled near the γ/γ' interfacial region to provide a free path for subsequent movement in γ matrix, {100} interfacial cracking occurred. As the crack moved away from the origin, fewer cycles were required to advance the crack due to the increasing crack size. The faster advancing rate subsequently resulted in lesser dislocation entanglement near γ/γ' interface and therefore cleavage on {100} planes was reduced or avoided.

LCF Double-Notch Testing

The LCF double-notch specimens fractured predominately by {111} planes in air and by {100} cleavage in hydrogen regardless of the maximum stresses. However, γ' pull-out was not observed in any of the DN-LCF specimens tested in hydrogen. The absence of γ' pull-out might be related to the maximum stress level and plastic strain. As shown in Table 5, the maximum stress level applied to the DN-LCF specimens is 100 ksi, which is lower than the yield strength. Therefore, the DN-LCF testing differed with the LCF smooth tests primarily in that gross yielding did not occur during the early cycles. The peak stresses at the start of cycling are greater in the smooth LCF strain-controlled tests. Thus the lack of γ' pull-out in DN-LCF specimens indicated that the hydrogen-induced fracture modes are very sensitive to the level of maximum stress. Because of the similarity in the fracture mode, the DN-LCF behavior can be explained using the same mechanism proposed for smooth LCF PWA 1489.

Conclusions

A high pressure gaseous hydrogen environment caused significant changes in fatigue crack initiation and propagation in PWA 1489. The evidence provided by the test results and fracture characteristics reached the following conclusions:

1) Hydrogen significantly reduced the fatigue life of PWA 1489 under all of the testing conditions and led to a substantial change in fracture mode.

2) The fractographic evidence supported the observation that hydrogen enhanced cleavage on {100} during the early stage of crack propagation. A very severe condition of such damage was evidenced by γ' pull-out near the LCF origin.

3) The occurrence of {100} cleavage was independent of the presence of grain boundaries and specimen geometries.

References

1) R.L. Dreshfield, and R.A. Parr, "Application of Single Crystal Superalloys for Earth-to Orbit Propulsion System", (AIAA/SAE/ASME/ASEE, 23rd Joint Propulsion Conference Proceedings, San Diego, California, June 29 - July 2, 1987).

2) P.S. Chen and R.C. Wilcox, "Fracture of Single Crystals of the Nickel-Base Superalloy PWA 1480E in Helium At 22°C", Metall. Trans, Vol. 22A, (1991), pp 731.

3) P.S. Chen and R.C. Wilcox, "Fracture of Single Crystals of the Nickel-Base Superalloy PWA 1480E in Hydrogen At 22°C", Metall. Trans, Vol. 22A, (1991), pp 2031.

4) P.S. Chen and R.C. Wilcox, "Hydrogen Induced Fracture Characteristic of Single Crystal Nickel-Based Superalloy", NASA Final Report, NAS8-38184 (1990).

5) C.L. Baker, J. Chene, I.M. Bernstein, and J.C. Williams, "Hydrogen Effects in [001] Oriented Nickel-Base Superalloy Single Crystals", Metall. Trans. Vol. 19A, (1988), pp 73-82.

6) M. Dollar and I.M. Bernstein, "The Effect of Hydrogen on Deformation Substructure, Flow and Fracture in a Nickel-Base Crystal Superalloy", Acta. Metall., Vol. 36, No. 8,(1988), pp 2369-2376.

7) R.K. Jacobs, "ATD Testing Program", IITRI Report No. IITRI-P06150-P333-1, (1990).

8) W.S. Walston, N.R. Moody, M. Dollar, I.M. Bernstein and J.C. Williams, The Effect of Hydrogen on the Deformation and Fracture of PWA 1480", Proc. Sixth Intl. Symp. on Superalloys, Duhl, D.N., Maurer, G., Antolovich, C., Lund, C., Reichman, S., eds. (AIME, Warrendale, PA, 1988), pp 295-304.

9) Pratt & Whitney, private communication, 1990.

10) K.S. Chan, J.E. Hack and G.R. Leverant, "Fatigue Crack Growth in MAR-M-200 Single Crystals", Metall. Trans. A, Vol. 18A, (1987), pp 581-591.

11) K.S. Chan, J.E. Hack and G.R. Leverant, "Fatigue Crack Growth in MAR-M-200 Single Crystals Under Multiaxial Cyclic Loads", Metall. Trans. A, Vol. 17A, (1986), pp 1739-1750.

12) L.G. Fritzemeire, and J.K. Tien, " The Cyclic Stress-Strain Behavior of Nickel-Base Superalloys-II Single Crystal", Acta. Metall., Vol. 36, No. 2, (1988), pp 283 - 290.

13) P.K. Wright and A.F. Anderson, " The Influence of Orientation on the Fatigue of Directional-Solidified Superalloys", Superalloys, (1980), pp 689-698.

14) P.S. Chen, "ATD Testing Program", IITRI Report No. IITRI-P06150-P411A, (1991).